New Developments and Challenges in Remote Sensing, Z. Bochenek (ed.)

Image-based correction of the aerosol effect over coastal waters with ASTER VNIR data

A.S.L. Nunes & A.R.S. Marçal
Faculdade de Ciências da Universidade do Porto, Porto, Portugal
Instituto Superior de Engenharia do Porto, Porto, Portugal

Keywords: aerosols, atmospheric correction, ASTER

ABSTRACT: The use of satellite remote sensing data for physical measurements of the Earth's surface requires the removal of the atmospheric contribution from the signal recorded at the sensor, a process usually called atmospheric correction. This task becomes more critical when the signal originating in the atmosphere dominates over the signal due to the surface itself, as is the case of remote sensing over ocean in the visible and near-infrared (VNIR), because of the very low water reflectance. A method is proposed to estimate the effects of the aerosols on the VNIR ASTER (Advanced Thermal Emission and Reflection Radiometer) bands 1 and 2, based on the selection of a suitable aerosol model (from a predefined set of candidates) and estimation of the aerosol optical thickness. This is achieved through the use of VNIR band 3 (760–860nm) dual-viewing geometry, for which the water-leaving reflectance is assumed to be null. The optical properties of the aerosol models are simulated using the 6S Radiative Transfer Code (RTC), which is also used to perform all the radiative transfer calculations. The method is described and tested with simulated ASTER data.

1 INTRODUCTION

Sensor bands located in the NIR are often used in ocean remote sensing for atmospheric correction purposes. Due to the strong absorption of liquid water, there is almost no radiation exiting the ocean, allowing the assessment of the atmospheric contribution to be done in this spectral range (Gordon, 1997). The effect of the atmospheric aerosols is usually the most difficult one to assess, due to the great variability of their distribution (both in space and time) and also to the wide diversity of their optical properties. There is usually a lack of data on aerosol composition and loading, for a given location and time, making the use of image-based methodologies effective to overcome the problem.

One of the main assumptions upon which this method is developed is the possibility of an image-based estimation of the aerosols contribution to the atmospheric radiative transfer. This is done by using two ASTER VNIR (Visible and Near Infrared) bands - band 3N (nadir viewing) and band 3B (backward viewing). Both bands have the same spectral range, and very similar spectral response functions (Yamagushi *et al*. 1998). Assuming that all other factors influencing the radiative transfer in the Sun-surface-sensor can be obtained from auxiliary data or estimated within acceptable accuracy, the aerosols optical thickness is retrieved from the joint use of the two ASTER VNIR bands

(3N and 3B). The most appropriate aerosol model is selected from a set of candidate models, based on the analysis of the aerosols scattering phase function.

The high spatial resolution (15m) of the ASTER VNIR data provides a useful tool for the assessment of the coastal waters and atmospheric properties. However, due to the low radiometric resolution of the ASTER VNIR sensor, its data are not usually used for ocean colour studies, where more sensitive sensors (e.g. MODIS, SeaWiFS) are required for the estimation of chlorophyll-a concentration, amongst other parameters (Gordon 1997). The sensor can nevertheless be suitable for applications such as the estimation of the amount of suspended sediments – the dependence of the water-leaving reflectance on the amount of suspended matter is a well-known fact in remote sensing (Doxaran *et al*. 2002). Although turbid coastal waters often exhibit some reflectance in the NIR, it is assumed that the requirement of null water-leaving reflectance still holds for the spectral range of ASTER VNIR band 3 (760–860 nm), unless the sediment load is extremely high (Wang & Gordon, 1994). The comparatively low radiometric resolution of the ASTER VNIR sensor helps holding the *null* water-leaving reflectance assumption for band 3.

The procedure presented here for ASTER is based on a single-band algorithm proposed for MISR (Multiangle Imaging SpectroRadiometer) data for the retrieval of the aerosol optical thickness over the oceans (Wang & Gordon 1994). Consequently, the same basic assumptions have to be met. The dual viewing geometry available for the ASTER VNIR band 3 (760–860 nm) is assumed to fit the requirements of the method: *null* (<1 Digital Count) water-leaving reflectance and observation of the same ground target area almost simultaneously from different viewing directions. For the consideration of multiple-scattering effects, the radiative transfer processes used for the aerosol contribution to atmospheric effects need to make use of aerosol models. The method performs a selection of the best aerosol model from a set of candidate models.

2 METHOD

A brief description of the bases and procedures of the method is presented here. A more thorough and detailed explanation may be found in Nunes (2005).

2.1 *The radiative transfer model*

The simplified Radiative Transfer Model (RTM) used is expressed by equation (1)

$$\rho_t = T_{og}\rho_r + T_{og}T_{\mathrm{H_2O}}\rho_a + T_{og}T_{\mathrm{H_2O}}T_s\rho_w \quad (1)$$

which is basically the same as what describes the RTM performed by the 6S (Second Simulation of the Satellite Signal in the Solar Spectrum) Radiative Transfer Code (Vermote *et al*. 1997). ρ_t is the total at-sensor equivalent reflectance, ρ_R is the reflectance resulting from multiple scattering by air molecules (Rayleigh scattering), ρ_a accounts for the multiple scattering by aerosols and the interaction between the Rayleigh and aerosols scattering and ρ_w is the water-leaving reflectance. $T_{\mathrm{H_2O}}$ stands for the water vapour transmittance, T_{og} for the transmittance of other gases, T_s for the total scattering transmittance and S for the spherical albedo of the atmosphere. All of the

transmittance terms in equation (1) are two-way transmittances, i.e. sun-target-sensor transmittances and the dependence on wavelength and geometry has been omitted for simplicity. ρ_R, T_{og} and T_{H_2O} can be obtained by assuming a standard atmospheric model – pressure, temperature, ozone and water vapour vertical profiles – such as the 6S embedded *midlatitude summer* model.

When using the proposed RTM in ASTER band 3, if assuming that the water-leaving reflectance is zero, the only term of equation (1) which depends on the aerosols is ρ_a. This parameter can then be estimated from the registered at-sensor reflectance ρ_t.

2.2 *Estimation of the aerosols optical thickness*

The possibility of estimating the multiple-scattering aerosol reflectance does not allow for itself the retrieval of the aerosol optical thickness. It is the aerosol single-scattering reflectance, ρ_{as}, that may be directly related with the aerosol optical properties – optical thickness τ_a, single-scattering albedo ω_a, and scattering phase function P_a (e.g. Gordon & Wang 1994)

$$\rho_{as}(\theta, \theta_0, \alpha, \lambda) = \frac{\omega_a(\lambda) P_a(\theta, \theta_0, \alpha, \lambda) \tau_\alpha(\lambda)}{4 \cos\theta_0 \cos\theta} \tag{2}$$

where λ is the wavelength, α is the scattering angle, and θ and θ_0 are the viewing and illumination angles, respectively.

For each aerosol model there is a near-linear relationship between the multiple-scattering and the single-scattering aerosol reflectance (Gordon & Wang 1994). Such relationships may be established, for each spectral band as a function of the viewing and illumination geometry.

The procedure proposed for the evaluation of the aerosol optical thickness and simultaneous selection of the most appropriate aerosol model with the ASTER VNIR band 3 is as follows. For each of the candidate aerosol models, it is assumed that both the single-scattering albedo and the scattering phase function are known. It is also assumed that one of these aerosol models will be closest (in terms of optical properties) to aerosols actually present in the atmosphere. Once the aerosol multiple-scattering reflectance is estimated from the at-sensor reflectance by equation (2), the aerosol single-scattering reflectance is determined by the linear relationship between the two quantities, for each aerosol model at each viewing geometry – nadir and backward. Next, the aerosol optical thickness for the *ith* model $(\mathrm{i} = 1, 2 \ldots \mathrm{N})$ at each viewing geometry $(\mathrm{j} = 1, 2 \ldots \mathrm{M})$ is derived using equation (2). For the *ith* aerosol model, the average optical thickness $<\tau_a^i(3)>$ and the corresponding standard deviation $\sigma_a^i(3)$ are computed. The aerosol model chosen as the most appropriate is that for which $\sigma_a^i(3)/<\tau_a^i(3)>$ is minimal. This criterion is based on the assumption that the use of an inaccurate aerosol scattering phase function will produce a wider dispersion of the $\tau_a^i(3)$ values estimated through equation (2). Therefore, the aerosol model chosen according to the minimisation of $\sigma_a^i(3)/<\tau_a^i(3)>$ is that whose phase function is closest to that of the actual aerosol (Wang & Gordon 1994).

The average optical thickness derived with the selected aerosol model is thus used as the correct estimation of the aerosol optical thickness for ASTER VNIR band 3. Within this image-based atmospheric correction method, the aerosol optical thickness in the

ASTER VNIR bands 1 and 2 is estimated based on the spectral dependence of the optical thickness of the selected aerosol model. The spectral behaviour of the aerosol optical thickness has to be determined for all the candidate aerosol models, which is done here using the 6S RTC. The aerosol optical thickness is computed for all three ASTER VNIR spectral bands and a relationship is established between the aerosol optical thickness in band 1 or 2 with that of band 3, allowing the estimation of $\tau_a^i(1)$ and $\tau_a^i(2)$ directly from the retrieved value of $<\tau_a^i(3)>$. These near-linear relationships depend on the aerosol model and may be computed using the 6S RTC. The information on aerosol composition (model) and loading (optical thickness) derived with the VNIR band 3 can be then used for the atmospheric correction of the visible bands.

2.3 *Atmospheric correction of ASTER VNIR bands 1 and 2*

The ASTER VNIR bands that are actually atmospherically corrected are bands 1 (520–600 nm) and 2 (630–690 nm) (Yamagushi *et al*. 1998), as the signal recorded by ASTER in band 3 is entirely attributed to the atmosphere, and is used only to assess the aerosol optical properties.

Once the aerosol optical thickness for the specific spectral band is known, the aerosol single-scattering reflectance is estimated using equation (2). The third and final step of the assessment of the aerosol contribution is the estimation of the aerosol-dependent terms on the radiative transfer equation (1) – the multiple-scattering aerosol reflectance and the total scattering transmittance. The assumptions about the aerosol model and optical thickness allow the estimation of ρ_a and T_s with the 6S RTC. The atmospheric vertical profiles of pressure, temperature, ozone and water vapour (from external data or atmospheric model) determine the values of ρ_R, T_{og} and $T_{\mathrm{H_2O}}$. The water-leaving reflectance in the ASTER visible bands is therefore retrieved by solving equation (1) where ρ_w is now the only variable to be determined.

3 TESTS

Simulated ASTER VNIR band 3 data were used here to guarantee the control over all the atmospheric characteristics. The use of actual ASTER data to first test the performance of the method would be possible only if external data on the optical characteristics of the aerosols, pressure, temperature, water vapour and ozone profiles were available. In the absence of such information it would not be possible to verify whether the method performs properly or not. Therefore, assuming null water-leaving reflectance for both ASTER bands 3, the 6S RTC was used to simulate the at-sensor reflectance, and all other radiative transfer terms required for the application of the method. The illumination and observation geometry parameters were set to the conditions of an ASTER image of the testing study area (Northwest coast of Portugal) acquired in 24/10/2001. The 6S RTC *midlatitude summer* atmospheric model was used to define the pressure, temperature, water vapour and ozone profiles. For the spectral range of this band, the aerosol optical thickness was allowed to vary between 0.01 and 0.80. The ρ_a versus ρ_{as} relationships are then obtained from the corresponding 6S simulated values, for each aerosol model and viewing geometry (nadir and backwards).

3.1 *Candidate aerosol models*

The aerosol types chosen to test the performance of this algorithm on ASTER data were those expected to be closest to the actual aerosols on the test area – a coastal zone that comprises a few urban centres, some industrial complexes and one main harbour: *Clean Maritime (CM), Maritime (M), Maritime Polluted (MP), Average Continental (AC)* and *Urban (U)* (d'Almeida *et al*. 1991, Levoni *et al*. 1997). The set of aerosol models used, whose optical properties were computed by the 6S RTC is formed by 40 aerosol models $(N = 40)$, which result from the five aerosol types with eight Relative Humidity (RH) levels each – 0, 50, 70, 80, 90, 95, 98 and 99%.

3.2 *Testing procedure*

For a definite aerosol optical thickness, an input aerosol model is used to define the aerosol conditions at which the at-sensor reflectance of ASTER band 3 is simulated by the 6S RTC. The respective multiple-scattering aerosol reflectance ρ_a is then computed using the RTM expressed by equation (1). For each of the N candidate aerosol models, the single-scattering aerosol reflectance is computed for the two viewing geometries, nadir and backward, using the appropriate ρ_a versus ρ_{as} relationships. Two values are obtained for the aerosol optical thickness, for each candidate model i: $\tau_a^i(3N)$ and $\tau_a^i(3B)$, with the nadir and backward viewing geometries, respectively. These two values are then used to calculate the average optical thickness $<\tau_a^i(3)>$ and the standard deviation $\sigma_a^i(3)$. The aerosol model selected is the one that minimises the quantity $\sigma_a^i(3)/<\tau_a^i(3)>$.

The purpose of the testing procedure is twofold. The first objective is the analysis of the consistency and accuracy of the selection criterion by using the same aerosol model simultaneously as input and candidate. If the method is consistent, it will select the same aerosol model that was used as input. The value of the optical thickness thus derived can be compared with the input value to assess the accuracy of the estimation. The second objective is the assessment of the stability of the method, i.e. the behaviour of the selection criterion when the actual aerosol characteristics are not strictly represented in the set of candidate models. This is achieved by analysing the aerosol model that would be selected in the absence of the correct one, and which is expected to be optically similar to the input model. This is an important issue, because in real situations, the aerosols actually present in the atmosphere will not always coincide with one of the candidate models.

All five aerosols types with six relative humidity levels – $RH = 50, 70, 80, 90, 95, 98\%$ – were used as input. Therefore, 30 aerosol models (*MC50* to *U98*) are used as input, and to each one of them all 40 aerosol models (*MC0* to *U99*) are included in the set of candidates. Three different values of aerosol optical thickness $(\tau_a = 0.1, 0.2, 0.4)$ at the spectral range of ASTER VNIR band 3 were used in each testing situation, thus yielding a total of 90 different input situations.

3.3 *Results*

3.3.1 *Illustrative example*

Figure 1 presents the results of the method in the selection of the best aerosol model. The value of the selection parameter $\sigma_a^i(3)/<\tau_a^i(3)>$ is plotted against the set of candidates aerosol models, for three (left plot) or five (right plot). The at-sensor equivalent

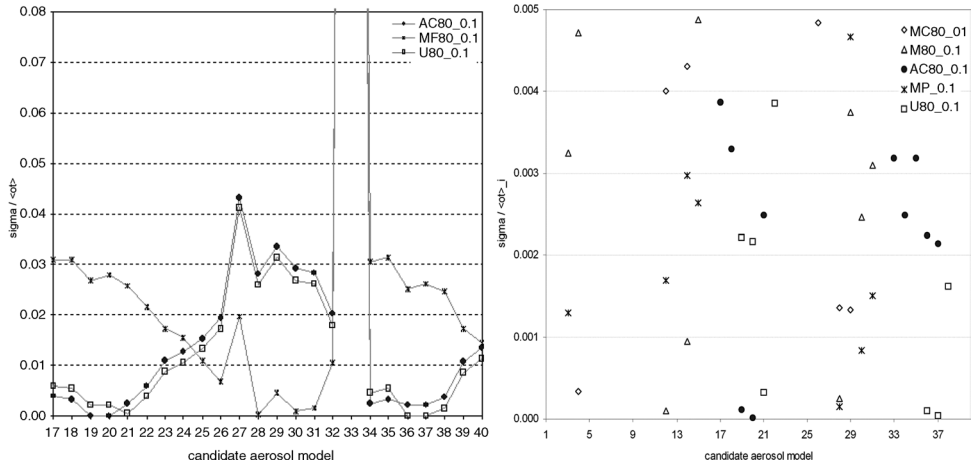

Figure 1. Analysis of the performance of the method in the selection of the best aerosol model, according with the minimisation of the selection parameter $\rho_a^i(3)/<\tau_a^i(3)>$ represented in the vertical axis. In the first plot (left), the input models are *AC80*, *MP80* and *U80* (#20, #28 and #36) and the set of candidate models is composed by the same three types with all RH levels. In the second plot (right), the input models are all types with RH $= 80\%$ (#8, #12, #20, #28 and #36) for the whole set of candidate models. τ_a was set to 0.1 and the aerosol models are sorted by type (*MC*, *M*, *AC*, *MP*, *U*) and then by ascendant RH level (0, 50, 70, 80, 90, 95, 98, 99%).

reflectance was simulated with an aerosol optical thickness of 0.1 and a relative humidity of 80%. All five aerosol types were used as input, and all 40 aerosol models were accepted as candidates. The subset shown in the first plot (left) refers to the *average continental*, *maritime polluted* and *urban* aerosol types. The plot shows a clear distinction in the performance of the 24 candidate models in the recreation of the input models. The most noticeable feature on a first sight is that the set of candidates behave in a very similar way in reproducing the *AC80* and *U80* aerosol models. On the other hand, the reproduction of the *MP80* model yields a set of values with a somehow opposite behaviour. This is because *AC80* and *U80* are aerosol models optically alike, being thus well reproduced by both *AC* and *U* aerosol types (with close RH values). As these two models are also very distinct from the *MP80*, the *AC* and *U* types do not represent well the *MP* type, and vice-versa. A more detailed analysis of the plot shows that the correct aerosol model is clearly selected for the input model *MP80*, with candidate no.28 being chosen – the same aerosol model as the input. For the *AC80*, the selection parameter is also minimised for the correct candidate model, #20, but almost ex-equo with #19 (*AC70*). When the input aerosol model is *U80*, the selected model is #37 (*U90*), instead of #36 (*U80*). However, the two candidate models yield almost the same value for the selection parameter. The aerosol optical thickness is estimated with less than 0.1% error for the first two cases, in which the correct aerosol model is selected. For the input model *U80*, the aerosol optical thickness is delivered by the selected *U90* model with an overestimation of about 10%.

The analysis of the stability of the method for this situation is quite illustrative of what happens when the correct model (or a very similar one) is not available. If the correct aerosol models were absent from the set of candidates, the minimisation of the selection parameter would lead to the choice of *AC70*, *MP95* and *U90* as best representing *AC80*, *MP80* and *U80*, respectively. Although these seem reasonable choices – *U90* is in fact chosen even in the presence of *U80* – the error in the estimation of the aerosol optical thickness is always above 10%, going up to 18% for the *AC* type.

A detailed view of a global selection (all the aerosol types are used both as input and candidate models) is shown in the second plot of Figure 1. Here, an extended view of the bottom of a general plot is provided, to emphasise the differences between the aerosols models that perform best in the recreation of the input models. As shown in the plot, all the input aerosol models converge to the corresponding aerosol type and most of them to the correct model (except the *U80*, as pointed out above). Both the *maritime clean* and *maritime* input aerosol models, *MC80* and *M80*, converge to the *maritime polluted* aerosol type when the correct aerosol model is not available in the set of candidates.

3.3.2 *Global results*

(1) *Consistency analysis*

The consistency of the method is evaluated by quantifying its convergence as the relative number of cases in which the selection criterion chooses the correct aerosol model.

A global analysis shows that in 73.3% of the cases tested, the method converges to the correct aerosol model, i.e., same aerosol type and relative humidity level. The best model comes in the second position for 22.2% of the cases, and in the third position for the remaining cases (around 4.4%). Considering only the cases in which the best aerosol model is not selected, the results show that 50.0% correspond to: (1) interchanges between the urban and average continental aerosol types with the same relative humidity level (25.0% of the cases), (2) selection of the same aerosol type with nearest RH (16.7%) or (3) interchange of urban and average continental aerosol types with nearest RH (8.3%). The remaining non-convergence cases (50.0%)are due to interchanges between the three maritime aerosol types or selection of the same aerosol type but with a different RH level. There is not a specific pattern perceivable for these cases.

To assess the existence of any specific trends of the convergence regarding the aerosol type, the RH level or the aerosol optical thickness, separate analysis were performed for each factor alone. It may be concluded that all the three factors have some influence on the convergence of the method, but none of them alone is crucial. The most determining factor was shown to be the aerosol type. For the *average continental*, *maritime clean* and *maritime polluted* types, in 83% of the cases the correct model is selected, followed by the *maritime* with 67% and the *urban* with a convergence rate of only 50%. The analysis of convergence of the method as function of the relative humidity level shows that the best results are obtained for RH $= 80\%$ and 95%, with a convergence rate of 87%, followed by RH $= 90\%$ with 73%, RH $= 70\%$ and RH $= 98\%$ with 67% and RH $= 50\%$ with a convergence rate of 60%. The input aerosol optical thickness has showed to be the less determining factor, with a convergence rate increasing with τ_a from 63% to 80%.

(2) *Stability analysis*

When the selected aerosol model was the same as the input, the aerosol optical thickness was retrieved with a negligible error (<0.1%). For the cases of interchange between the urban and average continental aerosol types with the same RH, or between two urban or average continental aerosol models, the estimation of the aerosol optical thickness is still accurate, with an error of less than 5%. However, the error in the estimation of the aerosol optical thickness goes up to around 10% for the less favourable situations – those in which both the aerosol type (*AC* or *U*) and relative humidity are not correctly estimated. On the remaining cases, the aerosol model that is chosen is not always optically similar to the input model, leading to aerosol optical thickness values that can be up to 40% in error when compared to the estimation which would have been done if the correct aerosol model had been selected.

4 CONCLUSIONS

The evaluation of the results could be made either with respect to the selection of the best aerosol model or with respect to the retrieval of the aerosol optical thickness in the ASTER VNIR band 3. Therefore, it is preferable that it is made separately for the case in which the input aerosol model is included in the set of candidate aerosol models, and for the case in which it is absent.

For the first case, the evaluation is based on the relative number of times the correct model is selected, and can be explored globally, by relative humidity level, aerosol type or input aerosol optical thickness. This part of the analysis is straightforward. For the number of cases in which the correct aerosol model is not selected, it is still possible to compare the value of the selection parameter, and verify whether it is close or not to the minimum.

When assuming that the input aerosol model is absent from the set of candidate models, the analysis of the performance of the method becomes much more complex. On a first thought, the error in the retrieval of the aerosol optical thickness in band 3 might present itself as a good analysis tool. However, such an analysis may turn out to be incomplete and biased. There are two reasons for that. The first is that when selecting an aerosol model different from that used as input, the estimated aerosol optical thickness will be necessarily different, because of the aerosol optical properties involved in its computation – aerosol scattering phase function and single-scattering albedo (see equation 2). Only in the case when the optical properties are very similar will the estimated optical thickness values be similar too. The other factor is related to the spectral dependence of the aerosol contribution. Since the main objective of the method is the assessment of the aerosol contribution (multiple-scattering reflectance amongst others) in the visible ASTER bands - VNIR bands 1 and 2 – it is important to assure that the correct spectral behaviour is being selected. Therefore, analysing only the error of the estimated aerosol optical thickness is not enough.

The results of the tests performed over simulated ASTER VNIR band 3 data show that for most of the situations, the correct aerosol model is selected whenever it is present as a candidate model. Most of the cases in which it is not selected correspond to

interchanges between the *urban* and *average continental* aerosol types with the same (or close) relative humidity levels. Those are in practise almost indistinguishable aerosol models, thus leading to accurate estimations of the aerosol optical thickness, as well as analogous spectral behaviours. However, there is a small number of cases when the selected aerosol model is not optically similar to the correct model, i.e. it does not produce the correct aerosol optical thickness at band 3 and its spectral behaviour will not allow an acceptable estimation of the aerosol contribution in the other spectral bands. Although this does not frequently occur, it can produce large errors in the atmospheric correction process.

As a result of the analysis of the method's performance, the conclusion is that the selection of the correct aerosol model has to be assured, for the atmospheric correction method to be reliable. Although that cannot be guaranteed, the use of a large number of aerosol models will certainly help overcoming the problem, increasing the probability that one of the candidate aerosol models is optically close to the actual behaviour of aerosols in the atmosphere. However, within such a testing procedure the method can only be partially evaluated, because only the aerosol model selection criterion and the retrieval of the optical thickness at the spectral range of ASTER VNIR band 3 are tested. It is not however possible to directly evaluate the consequences that a wrong selection of the aerosol model might have on the atmospheric correction of the ASTER visible bands.

Although further testing needs to be pursued, the proposed method shows to have potential to assist a radiative transfer code in the selection of a likely atmospheric aerosol scenario, which can contribute to a consistent atmospheric correction of the ASTER visible data over water.

ACKNOWLEDGMENTS

This work was done with the support of ''Centro de Investigação em Ciências Geo-Espaciais, Faculdade de Ciências da Universidade do Porto'', financed by ''Fundação para a Ciência e Tecnologia'' through POCTI/FEDER.

REFERENCES

d'Almeida, G.A., Koepke, P. & Shettle, E.P. 1991. *Atmospheric aerosols: global climatology and radiative characteristics*. A. Deepak Publishing.

Doxaran, D., Froidefond, J.M., Lavender, S. & Castaing, P. 2002. Spectral signature of highly turbid waters: application with SPOT data to quantify suspended particulate matter concerntration. *Remote Sensing of Environment* 81:149–161.

Gordon, H.R. 1997. Atmospheric correction of ocean colour imagery in the Earth Observing System era. *Journal of Geophysical Research* 102(D14):17081–17106.

Gordon, H.R. & Wang, M. 1994. Retrieval of water-leaving radiance and aerosol optical thickness over the oceans with SeaWiFS: a preliminary algorithm. Applied *Optics* 33(3):443–452.

Levoni, C., Cervino, M., Guzzi, R. & Torricella, F. 1997. Atmospheric aerosol optical properties: a database of radiative characteristics for different components and classes. *Applied Optics* 36(30):8031–8041.

Nunes, A.L. 2005. *Atmospheric correction algorithms for practical implementation on multispectral satellite images*. PhD Thesis, University of Porto.

Vermote, E.F., Tanré, D., Deuzé, J.L., Herman, M. & Morcrette, J.J. 1997. Second Simulation of the Satellite Signal in the Solar Spectrum, 6S: an overview. *IEEE Transactions on Geoscience and Remote Sensing* 35(3):675–686.

Wang, M. & Gordon, H.R. 1994. Estimating aerosol optical properties over the oceans with the Multiangle Imaging SpectroRadiometer: some preliminary studies. *Applied Optics* 33(18):4042–4057.

Yamagushi, Y., Kahle, A.B., Tsu, H., Kawakami, T. & Pniel, M. 1998. Overview of Advanced Spaceborne Thermal Emission and Reflection Radiometer (ASTER). *IEEE Transactions on Geoscience and Remote Sensing* 36(4):1062–1071.